The Astrophysical Journal, 674:247–257, 2008 February 10


# THREE-DIMENSIONAL OBSERVATIONS OF $H_2$ EMISSION AROUND SGR A EAST. I. STRUCTURE IN THE CENTRAL 10 pc OF OUR GALAXY

Sungho Lee,[1] Soojong Pak,[2] Minho Choi,[1] Christopher J. Davis,[3] T. R. Geballe,[4] Robeson M. Herrnstein,[5,6] Paul T. P. Ho,[5,7] Y. C. Minh,[1,7] and Sang-Gak Lee[8]

*Received 2006 July 24; accepted 2007 October 2*

## ABSTRACT

We have obtained velocity-resolved spectra of the $H_2$ 1–0 $S(1)$ ($\lambda = 2.1218$ $\mu$m) emission line at 2″ angular resolution (or ~0.08 pc spatial resolution) in four regions within the central 10 pc of the Galaxy where the supernova-like remnant Sgr A East is colliding with molecular clouds. To investigate the kinematic, physical, and positional relationships between the important gaseous components in the center, we compared the $H_2$ data cube with previously published $NH_3$ data. The projected interaction boundary of Sgr A East is determined to be an ellipse with its center offset ~1.5 pc from Sgr A* and dimensions of 10.8 pc × 7.6 pc. This $H_2$ boundary is larger than the synchrotron emission shell but consistent with the dust ring, which is believed to trace the shock front of Sgr A East. Since Sgr A East is driving shocks into its nearby molecular clouds, we can determine their positional relationships using the shock directions as indicators. As a result, we suggest a revised model for the three-dimensional structure of the central 10 pc. The actual contact between Sgr A East and all of the surrounding molecular material, including the circumnuclear disk and the southern streamer, makes the hypothesis of infall into the nucleus and feeding of Sgr A* very likely.

*Subject headings:* Galaxy: center — infrared: ISM — ISM: individual (Sgr A East) — ISM: lines and bands — ISM: molecules

## 1. INTRODUCTION

In the central 10 pc of our Galaxy, the Sgr A region contains several characteristic objects: a candidate for supermassive black hole (Sgr A*) of about $4 \times 10^6$ $M_\odot$ (see Ghez et al. 2003; Schödel et al. 2003 and references therein), a surrounding cluster of stars (the Central cluster), molecular and ionized gas clouds (the circumnuclear disk [CND] and Sgr A West), supernova remnants (SNRs G 359.92-0.09 and Sgr A East). They are surrounded by molecular structures including two giant molecular clouds (GMCs) M-0.02-0.07 and M-0.13-0.08 (also known as the 50 km s$^{-1}$ cloud and the 20 km s$^{-1}$ cloud, respectively). In addition to the two GMCs, recent accurate radio observations have resolved several dense and filamentary molecular features around the Sgr A complex: the molecular ridge, the southern streamer, the northern ridge, and the western streamer (see Fig. 1 of this paper, Figs. 3, 9, and 10 of McGary et al. [2001], and Fig. 14 of Herrnstein & Ho [2005]). These molecular features are believed to play important roles in feeding the central massive black hole (Ho et al. 1991; Coil & Ho 1999, 2000; McGary et al. 2001). The interaction between these various components is responsible for many of the phenomena occurring in this complicated and unique portion of the Galaxy. Developing a comprehensive picture of the primary interactions between the components at the Galactic center will also improve our understanding of the nature of galactic nuclei in general.

As the complicated morphology of the central 10 pc is being unveiled thanks to the dramatic progress of radio technology, efforts are being made to understand whether these features are really associated with the Galactic center or just seen along the line of sight in that direction, and to determine the relative positions of them along the line of sight, i.e., the three-dimensional (3D) spatial structure of the Galactic center.

Observations of 327 MHz absorption toward Sgr A West definitely place Sgr A East behind Sgr A West (Yusef-Zadeh & Morris 1987; see also Pedlar et al. 1989). Mezger et al. (1989) observed ring-shaped 1.3 mm dust emission surrounding Sgr A East across the 50 km s$^{-1}$ cloud and the 20 km s$^{-1}$ cloud, and suggested that Sgr A East has expanded into these molecular clouds. Based on these observational arguments, Mezger et al. (1989) proposed a 3D structure of the Sgr A complex and concluded that the event which created Sgr A East and the associated dust shell did not occur deep within the GMCs but close to their surfaces facing the Sun.

However, Geballe et al. (1989) found CO absorption toward a few Galactic center infrared (IR) sources and suggested that the 20 km s$^{-1}$ cloud may be located in front of Sgr A West. They also found some evidence that the 50 km s$^{-1}$ cloud lies partly in front of Sgr A West.

Based on the $NH_3$ morphology and kinematics observed using the Very Large Array (VLA), Coil & Ho (1999, 2000) located the Galactic nucleus (defined to include Sgr A*, Sgr A West, and the CND throughout this paper) behind the southern streamer (and the 20 km s$^{-1}$ cloud; see also Güsten & Downes 1980) and the 50 km s$^{-1}$ cloud (or the northern part of the molecular ridge) slightly behind Sgr A East. They also argued that the distance between Sgr A East and the 20 km s$^{-1}$ cloud along the line of sight should be smaller than 8.4 pc, which is the size of the

[1] Korea Astronomy and Space Science Institute, 61-1 Hwaam-dong, Yuseong-gu, Daejeon 305-348, South Korea.
[2] Department of Astronomy and Space Science, Kyung Hee University, Yongin-si, Gyeonggi-do 446-701, South Korea; soojong@khu.ac.kr.
[3] Joint Astronomy Centre, University Park, 660 North A'ohoku Place, Hilo, HI 96720.
[4] Gemini Observatory, 670 North A'ohoku Place, Hilo, HI 96720.
[5] Harvard-Smithsonian Center for Astrophysics, 60 Garden Street, Cambridge, MA 02138.
[6] Department of Astronomy, Columbia University, 550 West 120th Street New York, NY 10027.
[7] Academia Sinica Institute of Astronomy and Astrophysics, P.O. Box 23-141, Taipei, 106 Taiwan.
[8] Department of Astronomy, Seoul National University, Kwanak-gu, Seoul 151-742, South Korea.

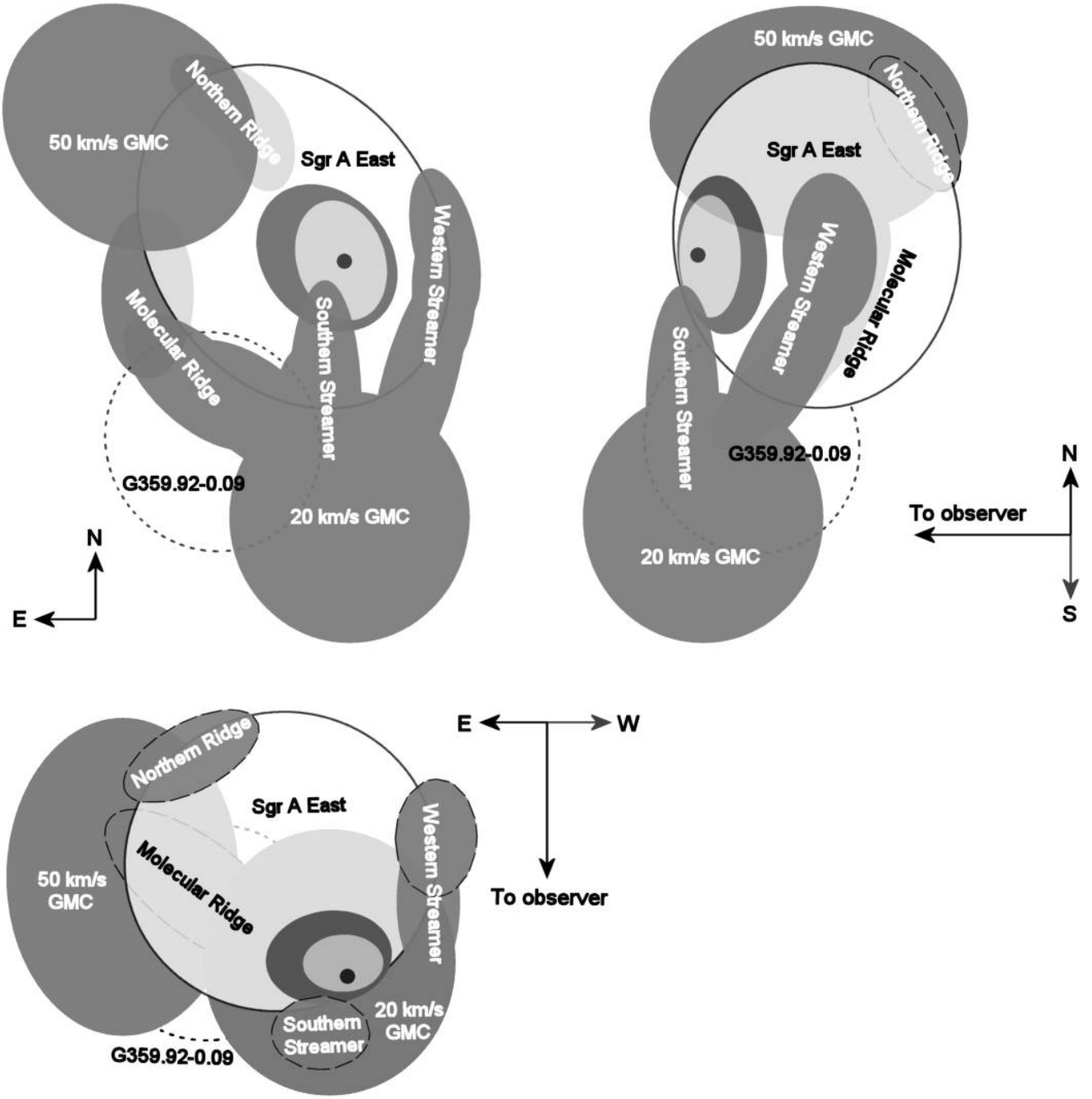


FIG. 1.— Schematic drawing of the 3D structure of the central 10 pc (the front, side, and top view in a clockwise direction). Black dots indicate Sgr A*. Sgr A West and the CND are simplified as two ellipses surrounding it. This model structure is based on the results of this work. See § 5 for details.

SNR G 359.92-0.09 in 20 cm radio continuum images (Yusef-Zadeh & Morris 1987; Pedlar et al. 1989).

Herrnstein & Ho (2005) updated and modified the 3D model of Coil & Ho (2000) based on their additional $NH_3$ line data and more recently published results (Maeda et al. 2002 and references therein; Park et al. 2004), as follows. The nuclear region is placed just inside the leading edge of Sgr A East. Only some part of the 50 km $s^{-1}$ cloud is located in front of the nucleus. The western streamer seen in $NH_3$ emission is highly inclined to the line of sight and is expanding outward with Sgr A East. The northern ridge is placed along the northern edge of Sgr A East and is expanding perpendicular to the line of sight. The southern streamer passes over the nucleus in projection but probably does not interact with it.

Together, the 3D models above agree on the following features.

1. The Galactic nucleus lies in front of Sgr A East but behind the southern streamer and part of the 20 km $s^{-1}$ cloud along the line of sight.
2. Sgr A East is expanding into the 50 km $s^{-1}$ cloud, the northern ridge, and the western streamer.
3. SNR G 359.92-0.09 is colliding with the southern part of the molecular ridge, the eastern edge of the 20 km $s^{-1}$ cloud, and the southern edge of Sgr A East.

On the other hand, contradictions among the models raise the following questions.

1. Is the nucleus in contact with or contained within Sgr A East?
2. Is the southern streamer falling into the nucleus?
3. Has Sgr A East expanded into the 50 km $s^{-1}$ cloud significantly, or just started to contact it?
4. Is Sgr A East colliding with the northern part of the molecular ridge?
5. Is Sgr A East in contact with the 20 km $s^{-1}$ cloud?
6. Is the 20 km $s^{-1}$ cloud located only in front of Sgr A East, or does it also extend further to the back side of it along the line of sight?

It should be noted that the models above are all based on indirect evidence, such as morphology, kinematics of molecular clouds, or absorption of background radiation by these clouds, rather than on direct, physical interactions between the objects. To answer some of the above questions directly, we have observed molecular hydrogen ($H_2$) emission and constructed a 3D picture of the Galactic center. $H_2$ emission is an excellent tracer of interactions between dense molecular clouds and other hot and powerful objects, such as Sgr A East.

In this paper we report observations of $H_2$ line emission from regions of interaction between Sgr A East and other gaseous components within the central 10 pc. Our observations were almost entirely of the $H_2$ 1–0 $S(1)$ line. Unlike most previous work, we observed this line at sufficiently high spectral resolution to resolve the velocity profiles and at high enough angular resolution to obtain detailed information on the spatial structure of the emission. We also obtained measurements of the $H_2$ 2–1 $S(1)$ line at 2.2477 $\mu$m at one location in order to investigate the excitation mechanism of the $H_2$.

We describe the observations in § 2 and the reduction of the spectroscopic data in § 3. Based on the directions of the shocks derived from the direct comparison of radial velocities with those from the $NH_3(3,3)$ data of McGary et al. (2001), we construct a 3D model for the structure of the central 10 pc in § 5. In a forthcoming paper we discuss the properties of the shocks and estimate the explosion energy and age of Sgr A East, from which we constrain its origin.

## 2. OBSERVATIONS

We surveyed four different fields in the $H_2$ 1–0 $S(1)$ line, near the edges of Sgr A East where interactions between its hot, expanding gas and molecular clouds in the central 10 pc are expected (see Fig. 2). The northeastern field (hereafter field NE) includes part of the 50 km $s^{-1}$ GMC and the northern ridge. The eastern field (field E) includes the northern portion of the molecular ridge. The southern field (field S) extends along the southern streamer, the northern half of which overlaps Sgr A East; 1720 MHz OH maser emission (an indicator of shock interactions) is also found in this field (Yusef-Zadeh et al. 1999a). The western field (field W) includes portions of the northwestern part of the CND and the northern part of the western streamer.

The data were obtained at the 3.8 m United Kingdom Infrared Telescope (UKIRT) during 2001 and 2003 using the facility instrument Cooled Grating Spectrometer 4 (CGS4; Mountain et al.1990) with its 31 lines $mm^{-1}$ echelle, 300 mm focal length camera, and a two-pixel-wide slit. The pixel scale along the slit was 0.90″ with the grating angle of 64.691° and the slit width on the sky was 0.83″. The angular resolution, which was affected by seeing and the optics of the spectrometer, was about 2″ (~0.08 pc at the distance to the Galactic center) based on the measured

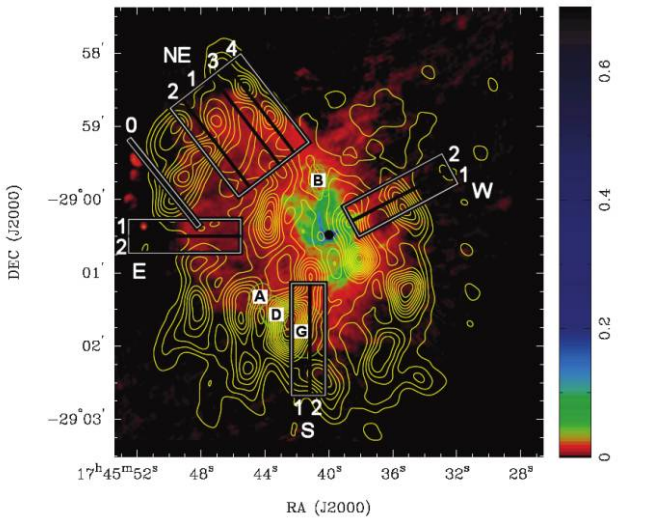


FIG. 2.—Field positions for the $H_2$ observations. The color image is the 6 cm continuum map of the central 10 pc (Yusef-Zadeh & Morris 1987) with $NH_3(3,3)$ emission contours superimposed from McGary et al. (2001). Sgr A East (*red shell*) surrounds Sgr A* (*black dot in the center*) and Sgr A West (*green and blue mini-spirals*) in the radio continuum. The four fields observed in $H_2$ 1–0 $S(1)$ using a slit-scanning technique are indicated by the labeled white boxes; these are the northeastern (NE; composed of 24 parallel positions of the 90″ length slit), eastern (E; 10 slit positions), southern (S; 10 slit positions), and western (W; 10 slit positions) fields. Each field is divided into two or four scanning blocks (labeled with numbers) by black solid lines. The narrow box (labeled 0) between field NE and field E is a supplementary field which is composed of only two slit positions and belongs to field E. This field (E-0) was observed to study the relationship between Sgr A East and compact H II regions in its eastern side, and the result will be reported separately. Contour levels are in intervals of 4 $\sigma$, where $\sigma = 0.33$ Jy $beam^{-1}$ km $s^{-1}$ (the beam size is ~15″ × 13″), and the scale bar ranges from 0 to 0.7 Jy $beam^{-1}$ (the beam size is 3.4″ × 3.0″). Letters A, B, D, and G mark the positions of OH (1720 MHz) masers (Yusef-Zadeh et al. 1999a).

FWHM of the flux profile of the standard star along the slit. The instrumental resolution, measured from Gaussian fits to telluric OH lines in our raw data, was ~18 km $s^{-1}$. The slit length was ~90″, which is longer than the typical size of a molecular clump of 30″ or 1.2 pc (see the $NH_3$ map in Fig. 2). CGS4 is a unique instrument in using such a long slit together with an echelle grating. Thus we could employ the observing technique of scanning large fields (similarly to the low-dispersion observations of Burton & Allen 1992; Lee et al. 2005) with the high spectral resolution.

Rectangular fields were observed by stepping the telescope by 3″ perpendicular to the slit axis. The telescope was nodded between object and blank sky positions every 20 minutes (one cycle for observing a single slit position consisted of one sky exposure and five object exposures) to allow subtraction of the background and telluric OH line emission. The sky positions were offset by about 2.5° ($\Delta\alpha = -2.03°$, $\Delta\delta = 0.85°$) from the on-source positions. We designate each slit position slit + [scanning direction] + [separation from a base position in the scanning block it belongs to; in arcseconds]. The base position is a starting point for scanning each field block and its coordinates are given in Table 1. For example, slit NW12 in field NE-1 is separated from the base position (called slit 00) by 12″ toward northwest. The integration time at each slit position was 1000 s. Two stars, HR 6496 (before 2003 May 28) and HR 6310 (on and after that date), were observed for flux calibration. The observations are summarized in Table 1.

The measurements on 2001 August 4 were performed slightly differently from those on other nights. In order to remove bad

TABLE 1
$H_2$ Observations with CGS4 and the echelle at UKIRT

| Field[a] | Date (UT) | Base Position[b] (J2000.0) R.A. | Decl. | Slit Names[c] (Number of Slits) | P.A.[d] (deg) | Seeing[e] (FWHM) (arcsec) |
|---|---|---|---|---|---|---|
| NE-1 | 2001 Aug 3–4[f] | 17 45 45.95 | −28 59 05.16 | NW15, NW12...SE12, SE15 (11) | 40 | 2.0 |
| NE-2 | 2001 Aug 4[f] | 17 45 45.86 | −28 59 06.54 | SE18, SE21, SE24 (3) | 40 | 2.1 |
| NE-3 | 2003 May 23 | 17 45 45.87 | −28 59 04.16 | NW15, NW18...NW24, NW27 (5) | 40 | 2.4 |
| NE-4 | 2003 May 28 | 17 45 45.95 | −28 59 05.16 | NW30, NW33...NW39, NW42 (5) | 40 | 1.8 |
| E-0 | 2001 Aug 4[f] | 17 45 50.60 | −28 59 44.30 | 00, SE03 (2) | 40 | 2.0 |
| E-1 | 2003 May 29 | 17 45 48.30 | −29 00 15.00 | 00, S03...S09, S12 (5) | −90 | 2.1 |
| E-2 | 2003 Jun 1 | 17 45 48.60 | −29 00 13.80 | S15, S18...S24, S27 (5) | −90 | 1.7 |
| S-1 | 2003 May 30 | 17 45 42.30 | −29 01 53.00 | 00, W03...W12, W15 (6) | 0 | 2.0 |
| S-2 | 2003 Jun 1 | 17 45 42.27 | −29 01 50.60 | W18, W21, W24, W27 (4) | 0 | 1.7 |
| W-1 | 2003 May 31 | 17 45 34.69 | −29 00 06.40 | 00, NE03...NE09, NE12 (5) | −60 | 2.2 |
| W-2 | 2003 May 31 | 17 45 34.80 | −29 00 05.00 | NE15, NE18...NE24, NE27 (5) | −60 | 2.2 |

Note.—For $H_2$ 1−0 $S(1)$ ($\lambda = 2.1218$ $\mu$m).
[a] See Fig. 2 for an outline.
[b] Base position for each slit-scanning block. Units of right ascension are hours, minutes, and seconds, and units of declination are degrees, arcminutes, and arcseconds.
[c] Defined by [scanning direction] + [separation from the base position in arcseconds].
[d] Position angle of slit (from north to east).
[e] Final spatial resolution on the detector, as produced by the natural seeing and optical system of CGS4.
[f] $H_2$ 1−0 $S(1)$ observations on 2001 August 4 (slit SE15 in field NE-1, field NE-2, and field E-0) using the slit-jittering method described in the text.

pixels more efficiently, the observing positions were jittered along the slit during the five exposures taken on each object ($\Delta p = 0$, +1, +2, −1, and −2 pixels in sequence).

## 3. DATA REDUCTION

The data were reduced in three stages. In the first stage, performed at the telescope by the UKIRT pipeline reduction software ORAC-DR, the individual frames were flat-fielded and approximately wavelength calibrated. The next stage involved the use of standard IRAF[9] routines to perform sky subtraction using the sky frames, interpolate over bad pixels, remove S distortions and wavelength distortion and impose an accurate (to $\pm 1$ km s$^{-1}$) wavelength calibration using OH lines. We also removed stellar continua and residual skylines, and flux calibrated using the spectra of HR 6496 and HR 6310. We determined the slit losses for these stars by assuming a circularly symmetric point-spread function (PSF) based on the flux profile along the slit length to estimate the missing stellar flux. The correction factor, which varies with the seeing, ranged from 2.06 to 2.94 (Lee & Pak 2006).

The final stage of data reduction involved the use of MIRIAD (Sault et al. 1995; Hoffman et al. 1996), a program package generally used for reduction and image analysis of radio interferometric data. However, MIRIAD can also be used for a general reduction of continuum and spectral line data. We employed MIRIAD to stack the two-dimensional spectral images into a single 3D data cube for each of the 11 fields (see Table 1) and then combined them into a total data cube that contains coordinate information for every position along every slit for each slit orientation. For more details see Lee (2005).

The resulting integrated intensity map for the combined data cube is shown in Figure 3. A smoothed version of the total cube, produced by convolving with a Gaussian profile of FWHM $= 3''$ to give a higher signal-to-noise ratio (S/N), is also presented in Figure 4.

## 4. $H_2$ EMISSION AROUND SGR A EAST

$H_2$ is the most abundant molecule in the interstellar medium (ISM). We cannot, however, observe $H_2$ directly in cold, dense molecular clouds because the lowest energy levels of $H_2$ are too high to be excited in these environments ($T < 50$ K). Instead, $H_2$ emission is observed in more active regions, for example in warm regions heated by shocks or in the surfaces of clouds illuminated by far-ultraviolet (far-UV) radiation. $H_2$ emission has been found associated with star-forming regions, SNRs, planetary nebulae, and active galactic nuclei.

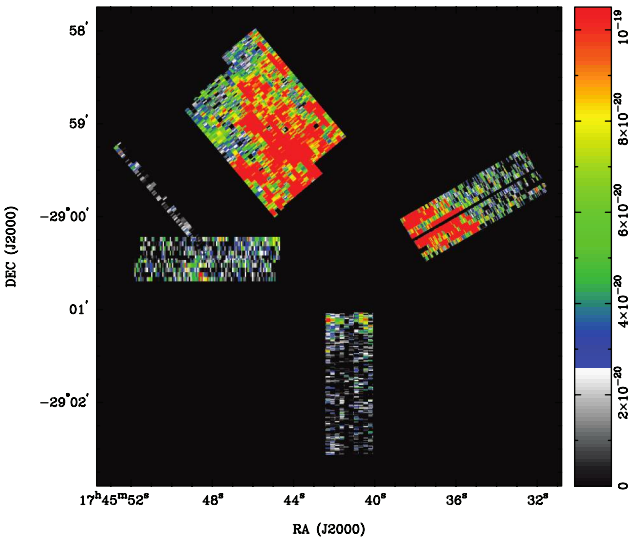


Fig. 3.—Velocity-integrated $H_2$ 1−0 $S(1)$ map of the entire surveyed region extracted from the combined data cube. The color-scaled intensity level is indicated by the side bar on the right in units of W m$^{-2}$ arcsec$^{-2}$.

[9] IRAF is distributed by the National Optical Astronomy Observatories, which are operated by the Association of Universities for Research in Astronomy, Inc., under cooperative agreement with the National Science Foundation.

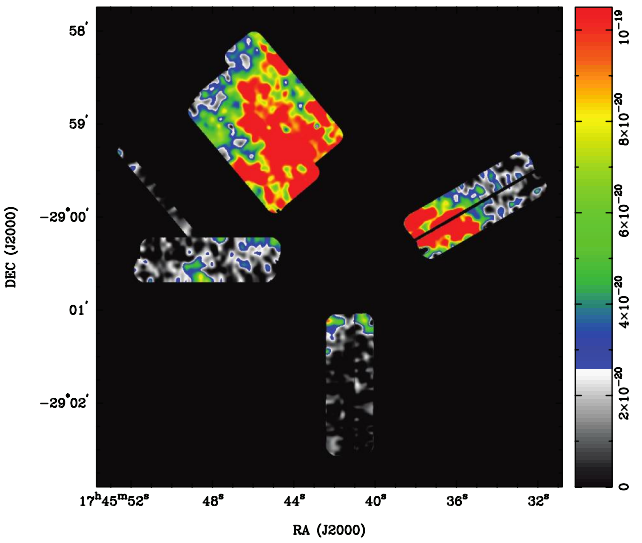


FIG. 4.—Velocity-integrated $H_2$ 1–0 $S(1)$ map of the entire surveyed region shown in Fig. 3, smoothed with a 3″ FWHM Gaussian. The color-scaled intensity level is indicated by the right-side wedge in units of W m$^{-2}$ arcsec$^{-2}$.

Since the first detection by Gatley et al. (1984) a number of groups have observed the Galactic center in $H_2$ line emission. Using a Fabry-Perot (FP) etalon, Gatley et al. (1986) mapped the CND in the 2.1218 $\mu$m $H_2$ 1–0 $S(1)$ emission with an angular resolution of 18″. They found that the CND has a broken, clumpy appearance. Burton & Allen (1992) obtained images in various emission lines [He I 2.058 $\mu$m, Br$\gamma$ 2.166 $\mu$m, and $H_2$ 1–0 $S(1)$] by scanning the telescope perpendicular to the slit, covering spatially an area of $103'' \times 145''$ and spectrally the entire K window (2.0–2.4 $\mu$m) with a resolution of $\lambda/\Delta\lambda = 400$. The near-IR images show a cluster of He emission line stars, the minispirals in Br$\gamma$, and the CND in $H_2$. They also observed the $H_2$ emission peak in the CND with normal spectroscopic techniques and suggested collisional fluorescence as the emission mechanism. On larger scales, Pak et al. (1996a, 1996b) surveyed the Galactic plane in the $H_2$ 1–0 $S(1)$ emission along a 400 pc strip. They found that $H_2$ emission can be seen throughout the surveyed region, peaking toward Sgr A. They also mapped the central 50 pc with a beam size of 3.3′ in diameter. Wardle et al. (1999) detected the $H_2$ 1–0 $S(1)$, 2–1 $S(1)$, and 1–0 $S(0)$ lines at the position A of the 1720 MHz OH maser detection in Figure 2. But they could not constrain the $H_2$ excitation mechanisms using line ratios because of large uncertainties in the line fluxes. Yusef-Zadeh et al. (1999b, 2001) also surveyed $H_2$ line emission around the regions where the OH masers have been detected, and imaged the CND and most of the Sgr A East region using NICMOS on the *Hubble Space Telescope* (*HST*). Their $H_2$ image has the highest spatial resolution (0.20″) obtained so far. To study the kinematics of the CND, they also observed this field using a FP etalon, with a FWHM spectral resolution of $\sim$75 km s$^{-1}$. Based on their results, combined with the OH detection, they suggested that the $H_2$ gas is shocked and accelerated by the expansion of Sgr A East into the 50 km s$^{-1}$ cloud and the CND.

Over the past two decades, in spite of dramatic advances in $H_2$ observations of the central 10 pc, there are still many remaining unsolved questions. The $H_2$ excitation mechanism is still in debate (UV heated vs. shock heated), particularly between studies using line ratios (Pak et al. 1996a, 1996b) and those based on the relationships with the OH masers (Wardle et al. 1999; Yusef-Zadeh et al. 1999b, 2001). The previous observations were concentrated on the CND, the brightest $H_2$ feature, rather than the regions where interactions between Sgr A East and the surrounding molecular clouds are expected. In addition, although the spatial resolution has greatly increased, the spectral resolution has not been high enough to investigate the detailed kinematics (e.g., line profiles) in the interaction regions. Considering that the widths of observed $H_2$ lines are generally less than 45 km s$^{-1}$, which is the critical velocity for shock dissociation in molecular clouds (e.g., Smith et al. 1991), the spectral resolutions (75–130 km s$^{-1}$) of previous spectroscopic observations with FP etalons (Gatley et al. 1986; Yusef-Zadeh et al. 1999b, 2001) are too low. To study the spatial and dynamical relationships between the various components in the central 10 pc, it is necessary to observe additional interaction regions other than the CND, in the $H_2$ emission at high spatial and spectral resolutions.

### 4.1. *Projected Morphology of Sgr A East in the* $H_2$ *Emission*

The morphology of Sgr A East has frequently been determined from the maps of 6 cm synchrotron radiation (Ekers et al. 1983; Yusef-Zadeh & Morris 1987; Pedlar et al. 1989; see Fig. 2). We investigate the morphology of the Sgr A East boundary in the $H_2$ emission, which is imaged for the first time in this study. Figure 5 shows our model of the Sgr A East boundary in projection based on the $H_2$ intensity map. The $H_2$ emission is significantly stronger than the rms noise of $5 \times 10^{-21}$ W m$^{-2}$ arcsec$^{-2}$ (the blue color represents roughly a 4 $\sigma$ detection) in most of the fields observed. The intense $H_2$ emission arises from the interaction regions related to the 50 km s$^{-1}$ cloud and the northern ridge in the northeastern field and from the regions related to the CND and the western streamer in the western field. In the eastern and southern fields, the $H_2$ emission is weaker.

An elliptical boundary is defined to trace the outer edges of the $H_2$ emitting regions with the center at $\alpha = 17^h45^m42.13^s$, $\delta = -29°0'8.6''$ (J2000.0), which is offset from Sgr A$^*$ by (+32″, +18″) or $\sim$1.5 pc at the distance of 8.0 kpc to the Galactic center (Reid 1993). The ellipse has a semimajor radius of $a = 135''$ ($= 2.25' = 5.4$ pc), a semiminor radius of $b = 95''$ ($= 1.58' = 3.8$ pc), and a position angle of 30° from north to east, which is almost parallel to the Galactic plane, whose position angle is $\simeq$34°. The elliptical boundary is determined qualitatively so that it can include all $H_2$ emission brighter than 10 $\sigma$ and be kept consistent in shape with the morphology in 6 cm continuum (Yusef-Zadeh & Morris 1987) and dust map (Mezger et al. 1989). This model of $H_2$ boundary might be revised by other studies since the model may depend on geometry or cloud structure as the $H_2$ emission arises only from local interface regions between Sgr A East and the clouds and our $H_2$ survey does not cover the whole region around Sgr A East.

The only conflict with this model is the southern field where the $H_2$ emission is situated well inside of the synchrotron shell in projection (compare Figs. 2 and 5). We suggest that this southern $H_2$ emission is not radiated from the southernmost edge of the Sgr A East shell but from a position where the tilted surface of the shell contacts a molecular cloud (i.e., the southern streamer) in front of or behind it. Alternatively, the $H_2$ emission may be extended more to the south from the detected position but severely diminished due to a very high extinction toward the southern part of the southern streamer (see the marginally detected $H_2$ emission in Fig. 12 where all the data in the southern field are summed to increase the S/N). Dust emission is strong in this direction (Zylka et al. 1998; see Fig. 9 of McGary et al. 2001) and the $NH_3$ opacity in this region is much higher ($\tau_{NH_3(1,1)} = 2$–5) than in the region where $H_2$ is detected ($\tau_{NH_3(1,1)} \ll 1$; see Fig. 2 of Herrnstein & Ho 2005). The 1720 MHz OH maser detected at

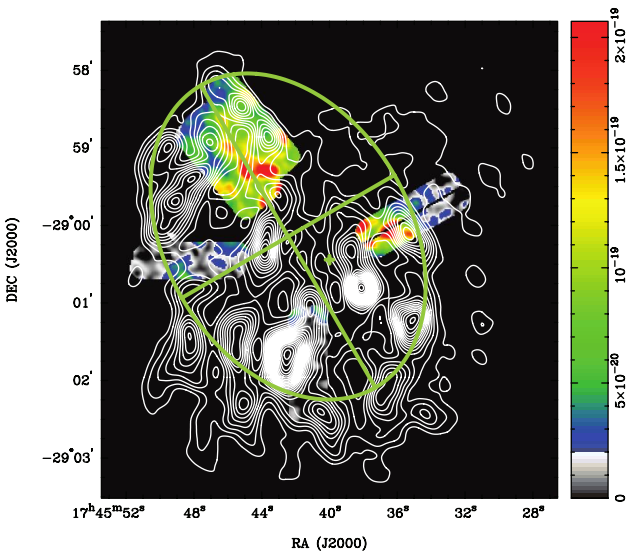


FIG. 5.—Definition of the Sgr A East boundary in $H_2$ emission. An ellipse defining the outer boundary of Sgr A East is overlaid on the integrated intensity map of $H_2$ 1−0 $S(1)$ line emission (smoothed by a Gaussian with FWHM = 5″) with contours for $NH_3$ (3,3) emission from McGary et al. (2001). The color-scaled intensity level is indicated by the right-side bar in units of W m$^{-2}$ arcsec$^{-2}$ and the contour levels are in intervals of 3 $\sigma$ (the rms noise $\sigma = 0.33$ Jy beam$^{-1}$ km s$^{-1}$ where the beam size is $\sim 15'' \times 13''$). The major and minor axes of the ellipse are also indicated; the plus sign at the center of the image represents the position of Sgr A*.

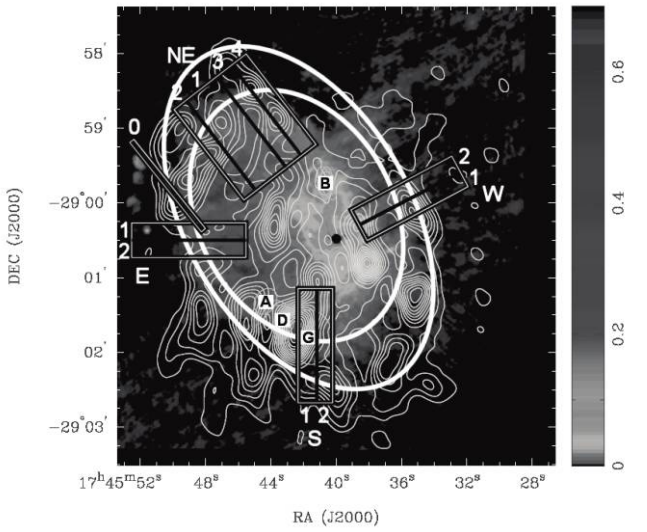


FIG. 6.—Two morphological models based on the 6 cm continuum map of Yusef-Zadeh & Morris (1987) (*inner ellipse*) and the dust map of Mezger et al. (1989) (*outer ellipse*) are superimposed on the gray-scale version of Fig. 2.

several positions around this region (see Fig. 2) by Yusef-Zadeh et al. (1996, 1999a) may support this hypothesis. Those authors interpreted the maser detections as indicators of shocks from Sgr A East toward its nearby molecular cloud, although Coil & Ho (2000) and Herrnstein & Ho (2005) argued that they originate from the interaction between Sgr A East and the SNR G 359.92-0.09. A similar interpretation is also possible for the 50 km s$^{-1}$ cloud. In the northeastern field of our $H_2$ observation, the $H_2$ intensity decreases toward the center of the 50 km s$^{-1}$ cloud (Fig. 5). In this direction the dust emission is the strongest in the central 10 pc and the $NH_3$ opacity is as high as in the southern streamer (Herrnstein & Ho 2005). Thus it is possible that, even though Sgr A East has expanded deeply into this cloud, the shock-excited $H_2$ emission is highly obscured.

Assuming the same center and the same position angle as our $H_2$ boundary, the projected 6 cm continuum shell can be simplified with an ellipse with $a_{6\,\mathrm{cm}} = 1.7' = 4.2$ pc and $b_{6\,\mathrm{cm}} = 1.3' = 3.0$ pc (Fig. 6). These dimensions are smaller than those of the $H_2$ boundary by about 20%. The boundary of Sgr A East defined by $H_2$ emission is more consistent with the dust ring observed by Mezger et al. (1989) than with the outer edge of the 6 cm shell. The partial ring of 1.3 mm dust emission surrounds the 6 cm synchrotron emission (see Fig. 3*b* of Mezger et al. 1989). This dust ring is well followed by the molecular clouds seen in $NH_3$ (see Fig. 6). The 50 km s$^{-1}$ cloud, the northern ridge, the western streamer, and the southern streamer in $NH_3$ emission are easily matched with the dust ridges. Assuming the same center and the same position angle with our $H_2$ boundary, the dust ring can be represented with an ellipse with $a_{\mathrm{dust}} = 2.5' = 6.0$ pc and $b_{\mathrm{dust}} = 1.5' = 3.7$ pc, which is nearly identical to the $H_2$ ellipse although the major axis of the dust ring is slightly (about 10%) longer.

In a comparison between their 1.3 mm map and the 6 cm map, Mezger et al. (1989) argued that the magnetic field of the synchrotron radiation is created in regions of the shell well downstream of the shock front. This argument, together with the fact that the dust ring coincides well with the outer boundary of the $H_2$ emission, implies that the $H_2$ boundary defined here actually traces the shock front of Sgr A East.

### 4.2. *Shock Interactions between Sgr A East and Molecular Clouds*

Lee et al. (2003) observed $H_2$ emission lines from interfaces between Sgr A East and both the 50 km s$^{-1}$ cloud (the GMC M-0.02-0.07) and the northern ridge. Based on the kinematics, they concluded that the $H_2$ molecules are excited by shocks from Sgr A East, although fluorescence works partially as well.

In this paper, large-scale spatial and kinematic structure of Sgr A East and the molecular clouds is investigated by comparing the position-velocity diagrams (PVDs) of the $H_2$ and $NH_3$ emission. The $H_2$ emission traces hot ($\sim$2000 K) gas and the $NH_3$ cool ($\lesssim$100 K) gas. In Figure 7 we superimpose the axes of the six PVDs shown in Figures 8–13. Each PV cut is selected to cover bright regions in both $H_2$ and $NH_3$ in general. More specifically, cut C1 is designated to pass through three $H_2$ emission peaks related to the 50 km s$^{-1}$ cloud and a $H_2$ emission feature around the northern end of the molecular ridge. Cut C2 is approximately along the northern ridge, which is curved toward the CND. To compare the 50 km s$^{-1}$ cloud and the northern ridge, cut C3 is laid across the two clouds and their related $H_2$ emission. Cut C4 goes along the whole length of the molecular ridge and the 50 km s$^{-1}$ cloud. The purpose of this cut is to study the relationships between these two clouds and the $H_2$ emission in this region. Similarly, cut C5 is made to pass through both the CND and the southern streamer in order to investigate whether the streamer is just a foreground feature as suggested by Herrnstein & Ho (2005). Finally, cut C6 goes across both the CND and the western streamer. This cut also covers a small patch of $H_2$ emission in the westernmost part (find more discussions on this $H_2$ feature in § 5.2).

In Figure 8, most of the $NH_3$ emission contours trace the 50 km s$^{-1}$ cloud and extend to the northern end of the molecular ridge (at positions $<-100''$). The small patch of emission at positions 10″–40″ and velocity of about 0 km s$^{-1}$ corresponds

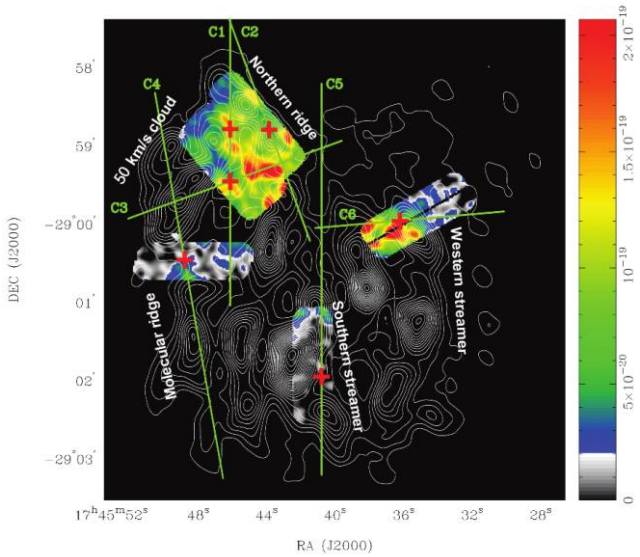


FIG. 7.—Positions of the cuts for the position-velocity diagrams (PVDs) of $H_2$ 1−0 $S(1)$ and $NH_3$ (3,3) emission in Figs. 8–13. For each cut, the labeled end indicates the direction of positive offset and the small plus sign corresponds to the reference position in each PVD. The $NH_3$ contours are labeled for the molecular clouds around Sgr A East. The $H_2$ 1−0 $S(1)$ map is smoothed by a Gaussian with FWHM = 5″. The intensity scale and contour levels are the same as Fig. 5.

to the northern end of the northern ridge. The $H_2$ emission observed in our northeastern field (at positions between −50″ and 50″) shows similar velocity peaks to $NH_3$. The velocity extension of $H_2$ is much broader, by as much as 60 km s$^{-1}$. This implies that strong shocks are propagating into the 50 km s$^{-1}$ cloud and the $H_2$ emission arises from turbulent postshock gas.

In the PVD for cut C4 (Fig. 11) which passes through the center of the molecular ridge along its length, we can see that the $H_2$ contours are broader in velocity and extend farther to the red side than $NH_3$. Thus we are certain that Sgr A East is in physical contact with and driving shocks into the molecular ridge too, at least into its northern part.

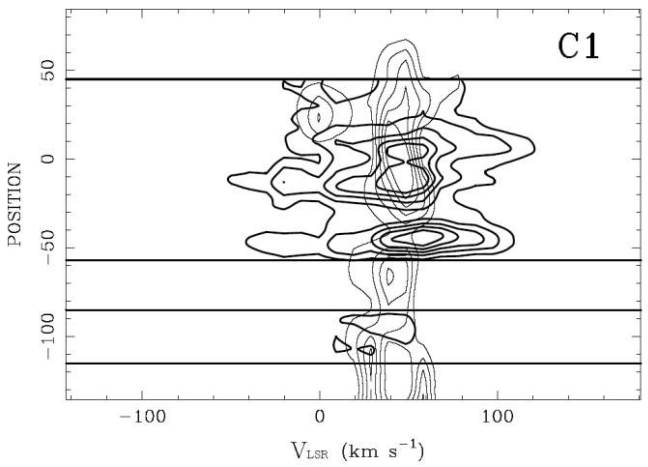


FIG. 8.—Position-velocity diagram for $H_2$ 1−0 $S(1)$ and $NH_3$ (3,3) emission along cut C1. Thick contours are for $H_2$ emission and thin contours are for $NH_3$. The contour levels are 2, 4, 6, 8, 10, 20, 40, 60, 80, and 100 $\sigma$ for both contours where $\sigma_{H_2} = 1.5 \times 10^{-22}$ W m$^{-2}$ arcsec$^{-2}$ km$^{-1}$ s and $\sigma_{NH_3} = 0.01$ Jy beam$^{-1}$. Positions in units of arcseconds are relative to the reference position which is marked on the cut in Fig. 7. Thick horizontal lines indicate the boundaries of the $H_2$ fields.

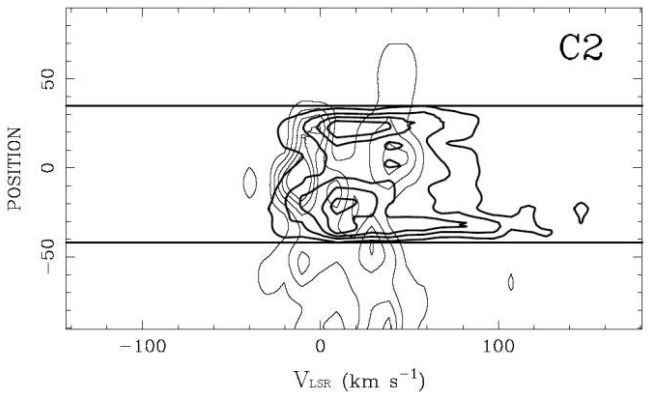


FIG. 9.—Same as Fig. 8 but for cut C2.

Cut C5 follows the southern streamer (see Fig. 12). The $NH_3$ at ∼+30 km s$^{-1}$ starts from −60″, continues through the nuclear region (between +90″ and +140″), and reaches beyond the northern boundary of the CND. The weak $NH_3$ features at both sides of the southern streamer (at 10, 60, and 80 km s$^{-1}$) are the satellite hyperfine lines of the strong main line (McGary & Ho 2002; Herrnstein & Ho 2005), and so have no additional kinematic meaning. The $NH_3$ feature with a very high velocity gradient between +40″ and +100″ is thought to be associated with the CND. In Figure 12, all cuts parallel to C5 in field S are combined to increase the S/N. The $H_2$ emission is clearly blueshifted with respect to $NH_3$ by at least 20 km s$^{-1}$ for both clouds. Thus the Sgr A East shock is also suspected to be the accelerator of the $H_2$ molecules in the southern streamer and the CND.

In Figure 13, the northwestern part of the CND is shown at positions >20″. The $NH_3$ emission from this cloud has a very broad velocity distribution (∼100 km s$^{-1}$) reflecting very complicated and energetic gas motions in the nuclear region. The related $H_2$ contours from 20″ to 30″ are as wide in velocity. The $NH_3$ emission contours here peak at ∼80 km s$^{-1}$ and are skewed toward positive velocities while the $H_2$ emission is peaked at ∼50 km s$^{-1}$ and is also bright toward lower velocities. This indicates that this part of the CND is located in front of Sgr A East and being pushed toward us by its expansion.

The second molecular feature in Figure 12 is the northern half of the western streamer at −30″ to 10″. The $H_2$ contours from the shocked gas at ∼0″ are as wide as ∼130 km s$^{-1}$ and extended slightly farther (by ∼30 km s$^{-1}$) both to the blue side and the red side than the $NH_3$. Thus it is likely that this part of the western streamer actually surrounds the western part of Sgr A East and

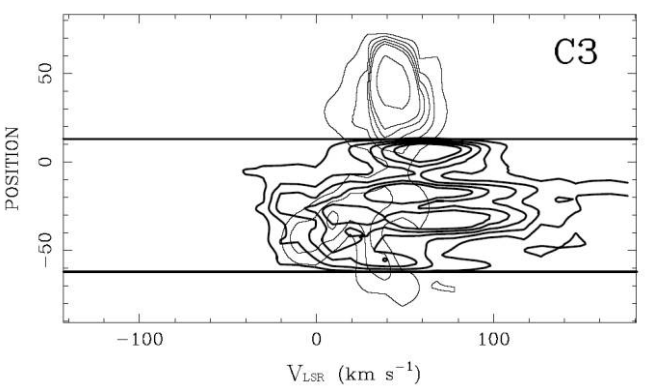


FIG. 10.—Same as Fig. 8 but for cut C3.

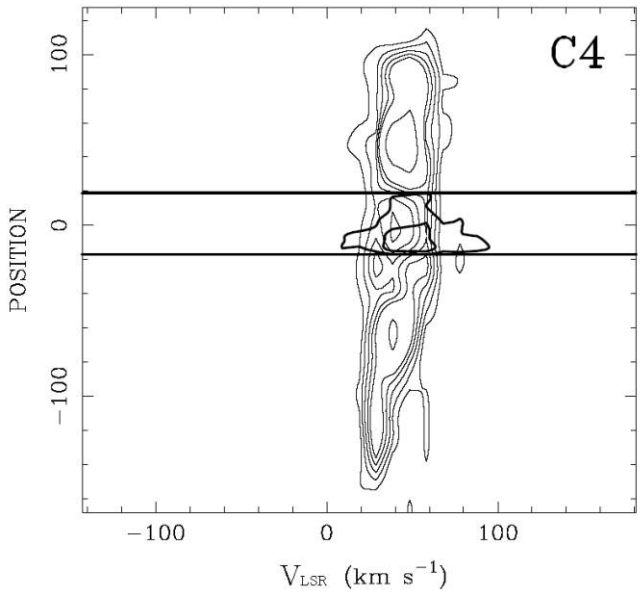


FIG. 11.—Same as Fig. 8 but for cut C4.

is being swept up by both the front and back of the expanding shell.

In summary, throughout the region, the $H_2$ emission lines are significantly broader than the $NH_3$ emission lines by a factor of 2–3. The $H_2$ profiles extend either blueward or redward of the $NH_3$, which traces the systemic (rest) velocity of each molecular cloud more accurately. This kinematics implies that the $H_2$ emission around Sgr A East clearly originates from shocks propagating into the molecular clouds (see Lee et al. [2003] for more detailed discussion on the $H_2$ excitation including partial role of nonthermal excitation).

## 5. 3D SPATIAL AND KINEMATIC STRUCTURE OF THE CENTRAL 10 pc

In this section we will discuss the features within the Galactic center region. Using our data and past observations (described below), we develop a 3D view of the region, which we show in Figure 1. Justification for the placement of the various components is given in the following subsections.

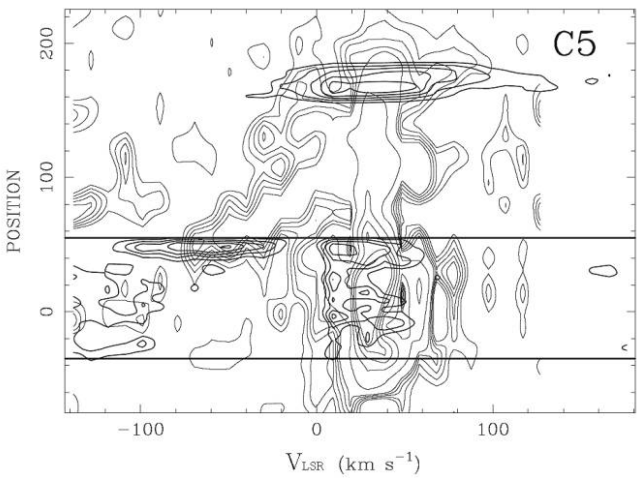


FIG. 12.—Same as Fig. 8 but for cut C5. All cuts parallel to C5 in field S are summed to increase the S/N. The broad $H_2$ contours at $\sim 170''$ are related to the 50 km s$^{-1}$ cloud and the northern ridge.

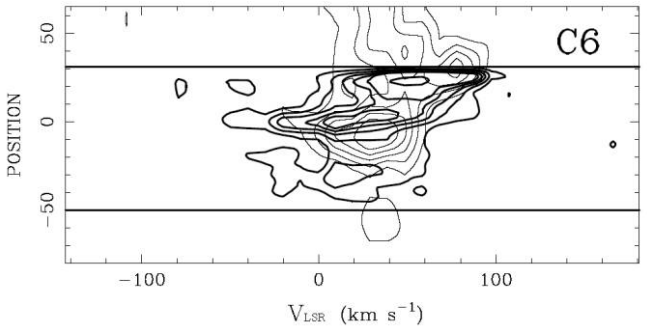


FIG. 13.—Same as Fig. 8 but for cut C6.

### 5.1. *Sgr A East as a Key Object in Understanding the 3D Structure*

Sgr A East surrounds the Sgr A* complex (including Sgr A West and the CND) in projection (see Fig. 2). Along the line of sight, absorption of nonthermal radiation is obvious evidence that the Sgr A* complex lies in front of the Sgr A East shell (Yusef-Zadeh & Morris 1987; Pedlar et al. 1989). A number of arguments, however, suggest that Sgr A* is in physical contact with or possibly embedded within the hot cavity of the Sgr A East shell (see Morris & Serabyn 1996; Yusef-Zadeh et al. 2000; Maeda et al. 2002 and references therein). For example, there exists faint nonthermal emission detected at 90 cm toward the thermally ionized gas although most of the nonthermal emission from Sgr A East is absorbed by the ionized gas associated with Sgr A West. This may indicate that Sgr A West is embedded in Sgr A East and the detected radiation is from the region between Sgr A West and the frontmost edge of the Sgr A East shell toward us (Yusef-Zadeh et al. 2000).

There is also observational support for the argument that Sgr A East is in physical contact with and driving shocks into the CND. Yusef-Zadeh et al. (1999b) found a linear filament of $H_2$ emission located at the western edge of the CND running parallel to the Sgr A East shell. This $H_2$ feature is thought to occur due to shock heating, as indicated by its morphology, the association with a source of 1720 MHz OH maser, and the lack of evidence for UV heating in the form of thermal radio continuum or Br$\gamma$ emission. In addition, a north-south ridge outlining the eastern half of the CND can be seen in the 20 cm continuum emission (Yusef-Zadeh et al. 2000). This elongated ridge is also detected at 90 cm (Pedlar et al. 1989; Yusef-Zadeh et al. 1999b), suggesting that it is a nonthermal feature related to Sgr A East. As we will see in § 5.2, Sgr A East is driving shocks into the northwestern part of the CND and accelerating the $H_2$ gas toward negative velocities. This interpretation supports the argument of Yusef-Zadeh et al. (2000) that the $H_2$ filament detected along the western edge of the CND is shock heated. Absorption features in $H_2CO$, OH, H I, and $HCO^+$ spectra with highly negative radial velocities ($V_{LSR} \simeq -190$ km s$^{-1}$) have also been observed toward Sgr A West (Marr et al. 1992; Pauls et al. 1993; Yusef-Zadeh et al. 1993, 1995; Zhao et al. 1995). The kinematics and spatial distribution of this gas place it at the Galactic center and Yusef-Zadeh et al. (2000) interpret its highly negative velocity as a result of acceleration by Sgr A East. Thus we conclude that Sgr A East is situated within the central 10 pc and that it is physically interacting with the Sgr A* complex.

Sgr A East is also actively interacting with the molecular clouds in the central 10 pc (McGary et al. 2001; Lee et al. 2003; Herrnstein & Ho 2005). In § 4.2 we demonstrate that Sgr A East is driving shocks into the surrounding clouds. As a result, we

can determine the relative locations of Sgr A East and the clouds in the line of sight based on the relative radial velocities between the shocked and unshocked gas. Hence Sgr A East is used as a key object in understanding the 3D structure around the nucleus of our Galaxy.

### 5.2. *Radial Velocities in* $H_2$ *and* $NH_3$. *Shock Directions and Spatial Relationships*

In § 4.2, Sgr A East is shown to be physically in contact with and driving shocks into all of the surrounding molecular clouds: the 50 km $s^{-1}$ cloud, the northern ridge, the molecular ridge, the southern streamer, the northwestern part of the CND, and the western streamer. In this section, we compare the velocity structures of the mutually related $H_2$ and $NH_3$ emission using the PVDs (Figs. 8–13) in order to determine shock directions and positional relationships along the line of sight between Sgr A East and the molecular clouds.

In Figure 8, the $H_2$ emission shows much broader velocity extension than the $NH_3$ contours of the 50 km $s^{-1}$ cloud, both to positive and negative velocities. This implies that strong shocks are propagating both toward us and in the opposite direction along the line of sight, within the 50 km $s^{-1}$ cloud. We can understand this if the western portion of the 50 km $s^{-1}$ GMC actually envelops Sgr A East, which is expanding into the cloud at both its front and back surfaces.

On the other hand, in Figure 8, the $H_2$ emission from the northern end of the molecular ridge has a narrow and very similar velocity distribution to the $NH_3$ emission. However, in Figure 11 for cut C4, which passes through the molecular ridge, the $H_2$ contours are broader in velocity and extend farther to the red side than $NH_3$. The velocity shift of $H_2$ here is about 20 km $s^{-1}$, which is much smaller than in the 50 km $s^{-1}$ cloud. However, considering that the molecular ridge is located at the outermost edge of the Sgr A East boundary and that its projected width is only about 1 pc, shocks from Sgr A East would propagate into the cloud nearly perpendicular to the line of sight and consequently the radial component of velocity shift of the shocked gas must be small. Nevertheless, we expect that the northern end of the molecular ridge is tipped slightly to the back side of Sgr A East since the $H_2$ emission there is redshifted, i.e., the hot cavity of Sgr A East is located in front of the ridge and pushing its material farther away from us.

As for the small emission patch of the northern ridge in Figure 8, it is difficult to distinguish between the $H_2$ emission that originated from this cloud and that from the 50 km $s^{-1}$ cloud since two molecular clouds overlap along the line of sight. This problem is similar to the other PVDs related to the northern ridge (Figs. 9 and 10 for cuts C2 and C3, respectively). However, there is a common aspect in these PVDs; there is no $H_2$ emission more blueshifted than the $NH_3$. This implies either that Sgr A East is located in front of the northern ridge along the line of sight or that the $H_2$ emission does not originate from shocked gas. The latter interpretation is not likely, as seen in § 4.2; in Figure 9, the positions of the bright peaks of broad (as much as 100 km $s^{-1}$) $H_2$ line emission are more closely coincident with two $NH_3$ peaks of the northern ridge (at $\sim$0 km $s^{-1}$) than with the single peak of the 50 km $s^{-1}$ cloud. Evidence for shocked $H_2$ emission in the northern ridge can also be found in Lee et al. (2003). Therefore we conclude that the northern ridge is located to the far side of Sgr A East and is being accelerated away from us.

In Figure 12 for cut C5, $H_2$ emission is only bright at $\sim$50″ but at two separate velocities of the southern streamer ($\sim$+30 km $s^{-1}$) and the CND (from $\sim-70$ km $s^{-1}$ to $\sim-10$ km $s^{-1}$). The $H_2$ emission is clearly blueshifted with respect to $NH_3$ by at least 20 km $s^{-1}$ for both clouds. Hence we conclude that Sgr A East is located behind the southern streamer and the southern part of the CND, respectively.

Figure 13 includes emission from three different molecular features. One is the northwestern part of the CND at positions >20″, where the $NH_3$ contours peak at $\sim$80 km $s^{-1}$. The related $H_2$ contours peak at $\sim$50 km $s^{-1}$ and are broadened toward lower velocities. This indicates that this part of the CND is located in front of Sgr A East and is being pushed toward us by its expansion. The second feature at $-30''$–$10''$ is the northern half of the western streamer. The related $H_2$ contours at $\sim$0″ are extended slightly farther (by $\sim$30 km $s^{-1}$), both to the blue side and the red side, than the $NH_3$. We interpret this as this part of the western streamer partially surrounding the western part of Sgr A East and being swept up by both the front and back of the expanding shell. The third feature is the $H_2$ emission at $\sim-35''$, which must certainly originate in shocked gas considering its wide velocity distribution of $\sim$80 km $s^{-1}$. It is not clear, however, from which molecular cloud it arises. Since its position is beyond the boundary of Sgr A East (Figs. 5 and 7), we cannot determine its line-of-sight position with respect to Sgr A East. This $H_2$ feature beyond Sgr A East may be associated with another phenomenon or accelerating source. For example, it might be a manifestation of the bipolar streamers or outflows from the Galactic nucleus which are suggested by radio and X-ray observations (Yusef-Zadeh & Morris 1987; Maeda et al. 2002). Or it might be shocked gas which has leaked out from the bubble (see the radio continuum feature toward northwest in Fig. 2). Further studies are needed to understand the nature and origin of this $H_2$ feature.

### 5.3. *3D Spatial Structure of the Central* 10 pc

In the previous sections, we presented a 3D model of the inner 10 pc of the Galaxy. Our model agrees with the previous studies (Mezger et al. 1989; Coil & Ho 2000; Herrnstein & Ho 2005) on the following points:

1. The Galactic nucleus lies in front of Sgr A East and behind the southern streamer and a part of the 20 km $s^{-1}$ cloud along the line of sight.
2. Sgr A East is expanding into the 50 km $s^{-1}$ cloud (M-0.02-0.07), the northern ridge, and the western streamer.

In addition to the above, we suggest the following:

1. Sgr A East is expanding deeply into the western edge of the 50 km $s^{-1}$ GMC, which envelops it both at the front and rear of the ionized shell.
2. The molecular ridge is approximately at the same distance as the center of Sgr A East, but the northern end of the ridge is tilted slightly to the back of it.
3. The northern ridge is in contact with the back side of Sgr A East.
4. The northernmost end of the southern streamer and the CND lie in front of Sgr A East and are being pushed toward us by it.
5. The northern part of the western streamer is located at the same distance as the center of Sgr A East and barely envelops the western edge of it.

Based on the outer boundary of the Sgr A East cavity defined by the $H_2$ line emission and above conclusions, we suggest a revised model for the 3D structure of the central 10 pc as shown in Figure 1.

## 6. CONCLUSIONS

Based on the $H_2$ emission map, we determine the outer boundary of Sgr A East where it is driving shocks into the surrounding molecular clouds to be approximately an ellipse with the center at (+32″, +18″) or ∼1.5 pc offset from Sgr A*, a major axis of length 10.8 pc, which is nearly parallel to the Galactic plane, and a minor axis of length 7.6 pc. This boundary is significantly larger than the synchrotron emission shell (Ekers et al. 1983; Yusef-Zadeh & Morris 1987; Pedlar et al. 1989) but is closely consistent with the dust ring suggested by Mezger et al. (1989).

Since Sgr A East is in physical contact with all of its nearby molecular clouds (the 50 km $s^{-1}$ cloud, the northern ridge, the molecular ridge, the southern streamer, the CND, and the western streamer), we are able to determine the positional relationships between Sgr A East and the molecular clouds along the line of sight using the shock directions as indicators. Based on the determined relationships and the strong evidence that Sgr A East is in contact with the nucleus, we suggest a revised model for the 3D spatial structure of the central 10 pc of our Galaxy modifying the previous models of Mezger et al. (1989), Coil & Ho (2000), and Herrnstein & Ho (2005).

Our conclusions on the 3D structure resolve most of the debates in previous studies as follows.

1. Is the nucleus in contact with or contained within Sgr A East? The Galactic nucleus is in physical contact with Sgr A East since the CND is pushed toward us by the expanding hot cavity of Sgr A East.

2. Is the southern streamer falling into the nucleus? It is highly probable that the southern streamer is falling into the nuclear region and feeding the CND. Sgr A East is driving shocks into the northernmost part of this cloud where it meets the CND in projection.

3. Has Sgr A East expanded into the 50 km $s^{-1}$ cloud significantly, or just started to contact it? In the $H_2$ data of the northeastern field, we can see that most of this region is filled with shocked gas from the 50 km $s^{-1}$ cloud. The area corresponds to at least one third of that of the entire cloud. Thus Sgr A East has significantly penetrated the cloud. If the cloud is wrapping around the Sgr A East shell with a casual morphological coincidence, however, the shocked layer might still be thin and on the surface.

4. Is Sgr A East colliding with the northern part of the molecular ridge? Yes, we detected shocked $H_2$ emission from the northernmost part of this cloud.

However, we cannot answer the questions related to the 20 km $s^{-1}$ cloud. We know the branches (the southern streamer and the western streamer) from this GMC are interacting with Sgr A East but the main body of this cloud is located far to the south, beyond the scope of our observations. Therefore the position and extent along the line of sight of this GMC in Figure 1 is uncertain. According to Coil & Ho (1999, 2000) SNR G 359.92-0.09 is expanding into the molecular ridge, the 20 km $s^{-1}$ cloud, and Sgr A East. Thus, if we observe the $H_2$ emission around SNR G 359.92-0.09 in a similar way to the 3D observations for Sgr A East, the questions about the 20 km $s^{-1}$ cloud could also be answered.

We thank the staff at UKIRT for their excellent support during our successful observations. Kind answers from Andy Adamson, Paul Hirst, and Tom Kerr concerning CGS4 were critically helpful for this work. Figure 2 is reproduced from Figure 10 of McGary et al. (2001) by permission of the AAS. The United Kingdom Infrared Telescope is operated by the Joint Astronomy Centre on behalf of the UK Particle Physics and Astronomy Council. T. R. G.'s research is supported by the Gemini Observatory, which is operated by the Association of Universities for Research in Astronomy, Inc., on behalf of the international Gemini partnership of Argentina, Australia, Brazil, Canada, Chile, the United Kingdom, and the United States of America. This work was supported by the Korea Science and Engineering Foundation (KOSEF) grant funded by the Korean government (MOST), R01-2005-000-10610-0.

## REFERENCES

Burton, M., & Allen, D. 1992, Proc. Astron. Soc. Australia, 10, 55
Coil, A. L., & Ho, P. T. P. 1999, ApJ, 513, 752
———. 2000, ApJ, 533, 245
Ekers, R. D., van Gorkom, J. H., Schwarz, U. J., & Goss, W. M. 1983, A&A, 122, 143
Gatley, I., Jones, T. J., Hyland, A. R., Beattie, D. H., & Lee, T. J. 1984, MNRAS, 210, 565
Gatley, I., Jones, T. J., Hyland, A. R., Wade, R., Geballe, T. R., & Krisciunas, K. 1986, MNRAS, 222, 299
Geballe, T. R., Bass, F., & Wade, R. 1989, A&A, 208, 255
Ghez, A. M., et al. 2003, ApJ, 586, L127
Güsten, R., & Downes, D. 1980, A&A, 87, 6
Herrnstein, R. M., & Ho, P. T. P. 2005, ApJ, 620, 287
Ho, P. T. P., Ho, L. C., Szczepanski, J. C., Jackson, J. M., & Armstrong, J. T. 1991, Nature, 350, 309
Hoffman, W., Hudson, J., Sharpe, R. K., Grossman, A. W., Morgan, J. A., & Teuben, P. J. 1996, in ASP Conf. Ser. 101, Astronomical Data Analysis Software and Systems V, ed. G. H. Jacoby & J. Barnes (San Francisco: ASP), 436
Lee, S. 2005, Ph.D. thesis, Seoul National Univ.
Lee, S., & Pak, S. 2006, J. Korean Astron. Soc., 39, 151
Lee, S., Pak, S., Davis, C. J., Herrnstein, R. M., Geballe, T. R., Ho, P. T. P., & Wheeler, J. C. 2003, MNRAS, 341, 509
Lee, S., Pak, S., Lee, S.-G., Davis, C. J., Kaufman, M. J., Mochizuki, K., & Jaffe, D. T. 2005, MNRAS, 361, 1273
Maeda, Y., et al. 2002, ApJ, 570, 671
Marr, J. M., Rudolph, A. L., Pauls, T. A., Wright, M. C., & Backer, D. C. 1992, ApJ, 400, L29
McGary, R. S., Coil, A. L., & Ho, P. T. P. 2001, ApJ, 559, 326
McGary, R. S., & Ho, P. T. P. 2002, ApJ, 577, 757
Mezger, P. G., Zylka, R., Salter, C. J., Wink, J. E., Chini, R., Kreysa, E., & Tuffs, R. 1989, A&A, 209, 337
Morris, M., & Serabyn, E. 1996, ARA&A, 34, 645
Mountain, C. M., Robertson, D. J., Lee, T. J., & Wade, R. 1990, Proc. SPIE, 1235, 25
Pak, S., Jaffe, D. T., & Keller, L. D. 1996a, ApJ, 457, L43
———. 1996b, in ASP Conf. Ser. 102, The Galactic Center, ed. R. Gredel (San Francisco: ASP), 28
Park, S., Muno, M. P., Baganoff, F. K., Maeda, Y., Morris, M., Howard, C., Bautz, M. W., & Garmire, G. P. 2004, ApJ, 603, 548
Pauls, T. A., Johnston, K. J., Wilson, T. L., Marr, J. M., & Rudolph, A. L. 1993, ApJ, 403, L13
Pedlar, A., Anantharamaiah, K. R., Ekers, R. D., Goss, W. M., van Gorkom, J. H., Schwarz, U. J., & Zhao, J. H. 1989, ApJ, 342, 769
Reid, M. J. 1993, ARA&A, 31, 345
Sault, R. J., Teuben, P. J., & Wright, M. C. H. 1995, in ASP Conf. Ser. 77, Astronomical Data Analysis Software and Systems IV, ed. R. A. Shaw, H. E. Payne, & J. J. E. Hayes (San Francisco: ASP), 433
Schödel, R., Ott, T., Genzel, R., Eckart, A., Mouawad, N., & Alexander, T. 2003, ApJ, 596, 1015
Smith, M. D., Brand, P. W. J. L., & Moorhouse, A. 1991, MNRAS, 248, 730
Wardle, M., Yusef-Zadeh, F., & Geballe, T. R. 1999, in ASP Conf. Ser. 186, The Central Parsecs of the Galaxy, ed. H. Falcke et al. (San Francisco: ASP), 432
Yusef-Zadeh, F., Lasenby, A., & Marshall, J. 1993, ApJ, 410, L27
Yusef-Zadeh, F., Melia, F., & Wardle, M. 2000, Science, 287, 85

Yusef-Zadeh, F., & Morris, M. 1987, ApJ, 320, 545
Yusef-Zadeh, F., Roberts, D. A., Goss, W. M., Frail, D. A., & Green, A. J. 1996, ApJ, 466, L25
———. 1999a, ApJ, 512, 230
Yusef-Zadeh, F., Stolovy, S. R., Burton, M., Wardle, M., & Ashley, M. C. B. 2001, ApJ, 560, 749
Yusef-Zadeh, F., Stolovy, S. R., Burton, M., Wardle, M., Melia, F., Lazio, T. J. W., Kassim, N. E., & Roberts, D. A. 1999b, in ASP Conf. Ser. 186, The Central Parsecs of the Galaxy, ed. H. Falcke et al. (San Francisco: ASP), 197
Yusef-Zadeh, F., Zhao, J. H., & Goss, W. M. 1995, ApJ, 442, 646
Zhao, J. H., Goss, W. M., & Ho, P. T. P. 1995, ApJ, 450, 122
Zylka, R., Philipp, S., Duschl, W. J., Mezger, P. G., Herbst, T., & Tuffs, R. 1998, in IAU Symp. 184, The Central Regions of the Galaxy and Galaxies, ed. Y. Sofue (Dordrecht: Kluwer), 291